THE PENNSYLVANIA STATE UNIVERSITY
SCHREYER HONORS COLLEGE

DEPARTMENT OF ELECTRICAL ENGINEERING

# OPTICAL DETECTION OF SMALL SIGNAL MAGNETIC FIELDS USING MAGNETOSTRICIVE CANTILEVERS

CHRISTOPHER CURWEN
Spring 2012

A thesis
submitted in partial fulfillment
of the requirements
for a baccalaureate degree
in Electrical Engineering
with honors in Electrical Engineering

Reviewed and approved* by the following:

Srinivas Tadigadapa
Professor of Electrical Engineering
Thesis Supervisor

Julio Urbina
Assistant Professor of Electrical Engineering
Honors Adviser

* Signatures are on file in the Schreyer Honors College.

# Abstract

Recent technologic developments have taken advantage of the magnetoelectric effect to build small signal magnetic field sensors with controlled detection of up to pico-Tesla magnetic fields. Many of these sensors are too large for certain applications, but promising designs for magnetoelectric resonant gate transistors that can be integrated with CMOS based signal processing circuits on a silicon substrate have shown nano-Tesla sensitivities and could potentially lead the way for smart sensor systems.

This honors thesis presents the optical characterization of the micro machined titanium/ Metglas® magnetostrictive cantilevers currently used in MERGT designs for the purpose of providing evidence of the functionality of the magnetostrictive cantilever as a tool for detecting magnetic fields. The noise characteristics of cantilevers and deflections of DC biased cantilevers in response to small signal magnetic fields are presented using two different experimental setups. The first setup uses the response of a position sensitive photo detector to a laser reflecting off the cantilevers, while the second setup uses a laser doppler vibrometer to directly measure the movement of the cantilevers. The following will provide a detailed description and evaluation of experimental setups and results of these optical measurements.

# Table of Contents

# List of Figures

# Acknowledgements

I would like to thank my thesis supervisor, Dr. Srinivas Tadigadapa. Dr. Tadigadapa welcomed me into his lab group as an undergraduate with no research experience and has patiently worked with me as I've learned the skills and methods required to work in experimental research. Dr. Tadigadapa has taught me much about the world of professional academia and research, which has proved to be invaluable information in helping me decide on a career path. I would also like to thank the graduate students in the Penn State MEMS lab, who have also taught me much about research and graduate student life: Kiron Mateti, Son Lai, Gokhan Hatipoglu, Duksoo Kim, Hwall Min, Pulkit Saksena, and Sharat Parimi.

I would also like to thank Dr. Suman Datta's graduate student, Feng Li. Feng provided many of the devices and experimental inspiration for the work presented in this paper. Additionally, he has personally helped me with many of my experiments and offered encouragement and advice when I became frustrated.

Finally, of course, I thank my parents, Pete and Diane Curwen, who have continually offered their encouragement and support of my academic pursuits since my first day of school.

# Chapter 1: Introduction

## 1.1 Magnetic Sensors

Magnetic sensing technology has played a significant role in applications such as detection of direction, rotation, angle, or electrical current. The technology for magnetic field sensing has been driven by the need for improved sensitivity, smaller size, and compatibility with electronic systems. Detection of both small and large magnetic fields has important uses, but very few magnetic sensors are designed to sense both small and large fields. Most sensors are designed for high accuracy in a specific range of magnetic field strength [1]. Figure 1.1 demonstrates the variety of magnetic sensors in use today and they're variable field detection ranges.

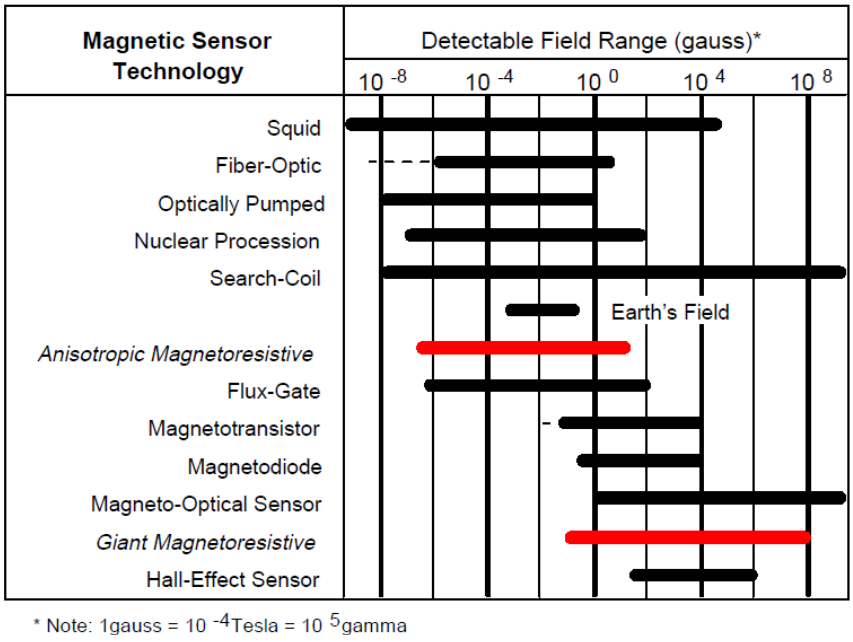


**Figure 1.1.** A list of magnetic sensing technologies and their respective ranges of sensitivity. Taken from [1].

In this thesis, we are primarily concerned with small field sensors. Small field sensors are important for use in medical applications such as detecting the neuromagnetic field generated by the brain, and military surveillance applications. As seen in Figure 1.1, the Superconducting Quantum Interference Device (SQUID) is commonly recognized as the

most sensitive sensor type available. Unfortunately, most SQUID devices either require cryogenic refrigeration and/or are too large for medical applications [2].

One promising technology being developed uses a magnetoelectric resonant gate transistor (MERGT) to achieve nanotesla sensitivities. The MERGT uses a resonant gate in the form of a magnetostrictive cantilever located atop a sensing and amplifying transistor. As the magnetostrictive cantilever reacts to an applied magnetic field, the air-gap capacitance is modulated, causing a modulation of the channel charge density of the field effect transistor (FET), which finally leads to a modulation of the FET's drain current [3]. The characterization of this magnetostrictive resonant gate is presented in this thesis. Figure 1.2 provides a schematic of the MERGT structure and function.

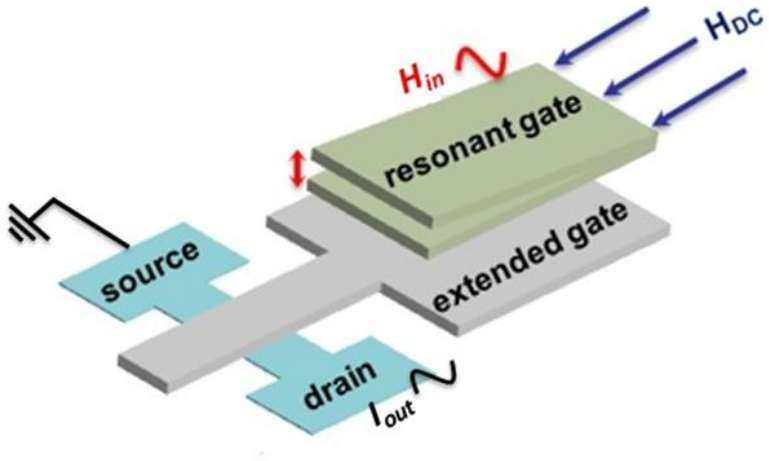


**Figure 1.2.** Illustration of structure and functionality of a MERGT magnetic sensor. Taken from [3].

## 1.2: Magnetostriction

Magnetostriction is a property of ferromagnetic materials that causes their physical dimensions to change in response to an applied magnetic field. Magnetostrictive materials are divided up into individual magnetic domains that are randomly oriented. When a magnetic field is applied to a magnetostrictive material, the force on the domains results in a shifting of domain boundaries and rotation of domain alignment. This shifting and rotating of domains results in physical stress that manifests itself as a change

in the physical dimensions of the material. All magnetostrictive materials have a saturation field at which the physical dimensions of the material cannot change anymore with an increased magnetic bias.

## 1.3: Magnetostrictive Materials

Magnetostrictive materials are typically characterized by their magnetostrictive coefficient, which is defined as the fractional change in length as the applied magnetic field increases for zero to saturation value. Magnetostrictive materials are also characterized by the change in the Young's modulus of the material that results from the elastic strain associated with the deformation caused by a magnetic bias [4].

Cobalt has a magnetostrictive coefficient of 60 microstrains, which is the largest magnetostrictive coefficient of any pure element. However, much larger magnetostrictive coefficents can be obtained in alloys. Two of the most common alloy magnetostrictive materials include Terfenol-D ($Tb_xDy_{1-x}Fe_2$) and Meglas ($Fe_{81}Si_{3.5}B_{13.5}C_2$). At a value of 2,000 microstrains, Terfenol-D has the largest magnetostrictive coefficient of any known material, however, Terfinol-D is very magnetically anisotropic and so requires a very large magnetic bias of 160 kA/m to drive the magnetostriction to saturation. Metglas®, on the other hand, only has a magnetostrictive coefficient of 20 microstrains, however, it only requires a magnetic bias of 1 kA/m to drive it to saturation [5].

## 1.4: Magnetostrictive Unimorph

A magnetostrictive unimorph is a cantilever structure that uses one active layer (the magnetostrictive layer) and one passive layer. In this thesis, we are studying a magnetostrictive unimorph composed of a 500 nm passive layer of titanium and a 150 nm active layer of Metglas®. Metglas® was selected as the magnetostrictive material for this unimorph because of its high saturation magnetostriction coefficient (as explained in section 1.3). A plot of the magnetostrictive coefficient versus the applied magnetic field is shown in Figure 1.3. Additionally, Metglas® shows a reduction of the effective

Young's modulus of up to about 80% under saturation conditions. This allows for a more energy-efficient unimorf.

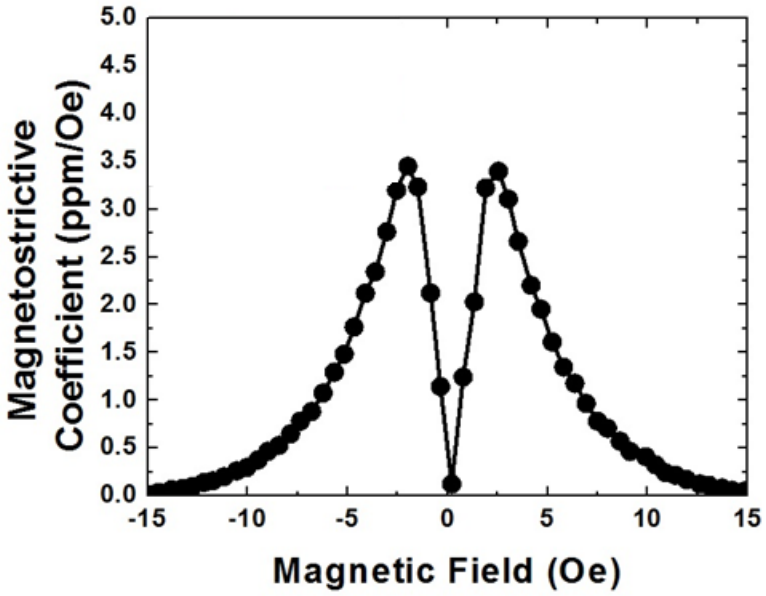


**Figure 1.3.** A plot of the magnetostrictive coefficient of Metglas® as a function of applied magnetic field. Taken from [6].

Using the characteristics of Metglas® and the dimensions of the Ti/ Metglas® unimorf, the deflection of the unimorf is described by the following equation:

$$deflection = \frac{3l^2}{t_m} \frac{AB(B+1)}{A^2B^4 + 2A(2B + 3B^2 + 2B^3) + 1} d_{31}^m H_{ac}$$

where

$$A = \frac{E_p}{E_m}$$

is the Young's modulus ratio ($E_p$ is the Young's modulus for Ti, and $E_m$ is the Young's modulus for Megtlas), and

$$B = \frac{t_p}{t_m}$$

Is the thickness ratio (where $t_p$ is the thickness of the Ti, and $t_m$ is the thickness of the Metglas®), $d_{31}{}^m$ is the magnetostrictive coefficient, and $H_{ac}$ is the AC magnetic field. Theoretical and experimental verification of the deflection of the unimorf is demonstrated

in Figure 1.4. In this figure, capacitance is shown as a function of applied magnetic field, but capacitance is proportional to distance between the cantilever and substrate, which is proportional to the cantilever's deflection.

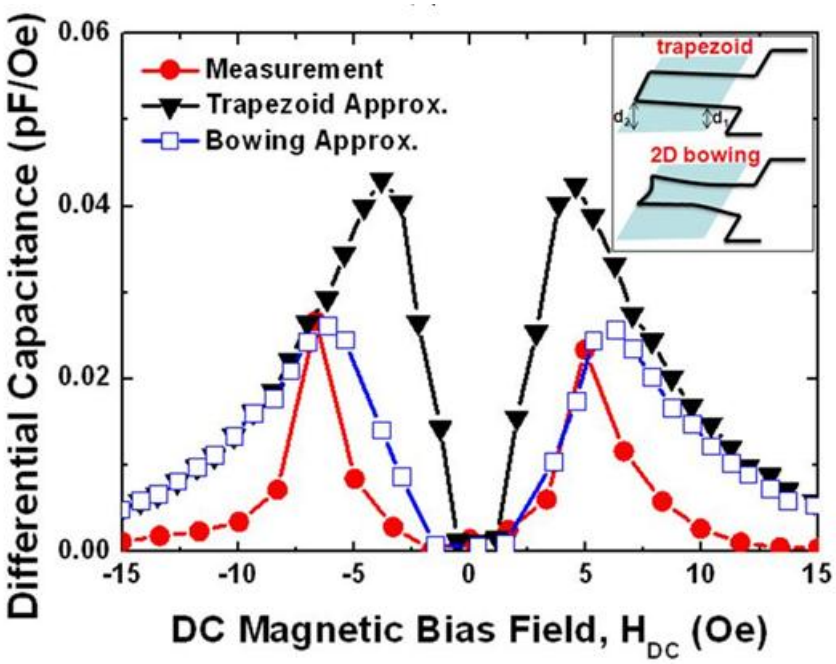


**Figure 1.4.** Plots of theoretical and experimental verification of the cantilevers deflection as a function of applied magnetic field. Taken from [6].

# Chapter 2: MEMS Cantilevers

## 2.1 Cantilever Transducers

Microelectromechanical Systems (MEMS) are frequently used as transducers that convert a physical quantity into a readable signal. MEMS cantilevers are one of the most common MEMS devices and are suitable as transducers of physical, chemical, and biological stimuli. The MEMS cantilever is based around the simple idea that such stimuli can affect the mechanical characteristics of the cantilever, and these effects can readily be measured and converted into a readable signal. Typically the effect on the cantilever is observed as either a physical deflection, a shift in resonant frequency [7]. Examples of transduction mechanisms involved in cantilever sensors are shown in Figure 2.1.

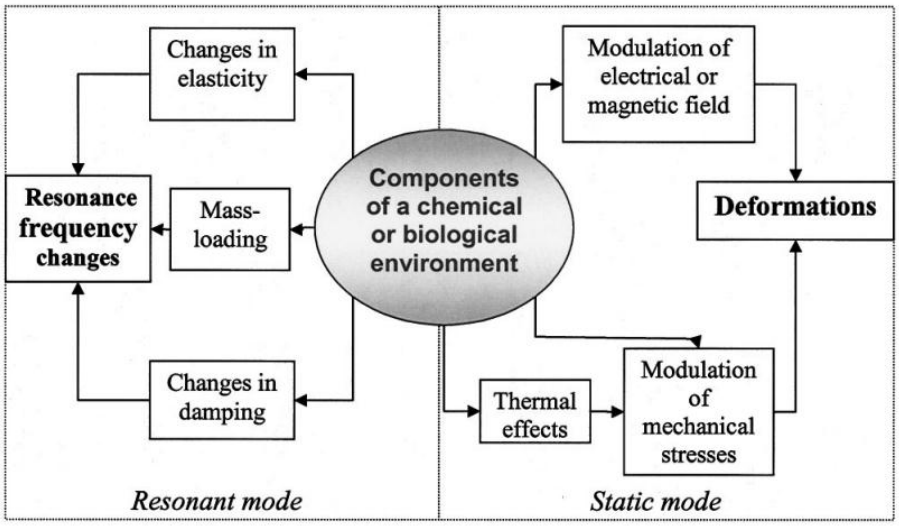


**Figure 2.1.** Flow chart showing examples of transduction mechanisms involved in cantilever sensors. Taken from [7].

## 2.2 Methods of Cantilever Readout

In order to use a MEMS cantilever transducer, you must have both a cantilever that responds to the desired stimuli and a method for real-time measurement of this response.

The following are common methods used for detecting changes in cantilever devices:

- Optical methods:
    - Optical beam deflection: a laser diode is reflected off the surface of the cantilever and the movement of this reflected laser is monitored by a position sensitive photodetector.
    - Optical interferometry: a laser is reflected off the surface of a cantilever and acquires a slight shift in frequency due to the Doppler effect when the cantilever moves. The interference of the incident and reflected beam is dependent on this Doppler shift and can be used to measure the movement of the cantilever.
- Peizoresistance method: a change in resistance can be measured when a doped silicon cantilever is deformed.
- Piezoelectric method: a piezoelectric layer that is deposited on a cantilever can show an accumulation of charge in response to the deformation of the cantilever.
- Capacitance method: the capacitance between a cantilever and substrate can be measured and shows a dependence on the gap between the cantilever and substrate.
- Electron tunneling: if a subnanometer gap exists between the tip of a cantilever and a surface, an electron tunneling current can be measured by apply a voltage bias between the tip and the sample. The tunneling current is highly dependent upon the gap between the cantilever and the sample.

Each method for detecting cantilever responses has its own advantages and disadvantages. For example, optical methods do not require electrical contacts, as the other methods do. On the other hand, optical methods can be sensitive to the media surrounding the cantilever, which may not pose a problem for the other techniques [7]. In this thesis, we are focused on using optical methods for characterizing the static deflections of magnetostrictive cantilevers, however, when used in the MERGT device, a FET is used to readout the changes in the magnetostrictive cantilever's resonant frequency.

# Chapter 3: Results

## 3.1: Description of Cantilever Devices

The titanium/ Metglas® cantilevers developed by Feng Li were fabricated using a surface micromachining process. A 500 nm layer of amorphous silicon was used as the sacrificial layer, and a window patterning with dimensions of 500 µm × 100 µm was used as a lift off mask for the cantilever. Next, 500 nm of titanium was deposited using a sputtering process, followed by the deposition of 100 nm of Metglas® using a sputtering process. Again, a 600 oersted DC magnetic bias was used to align the magnetic domains of the Metglas®. A lift off lithography process was used to release the cantilevers, followed by $XeF_2$ dry etching and annealing at 350ºC to further define the cantilevers and release internal stress. Still, Zygo measurements reveal that the cantilever was bending up by 5 µm due to the stress mismatch between deposited layers [3]. An image of the titanium/ Metglas® cantilever used in the MERGT device is shown in Figure 3.1.

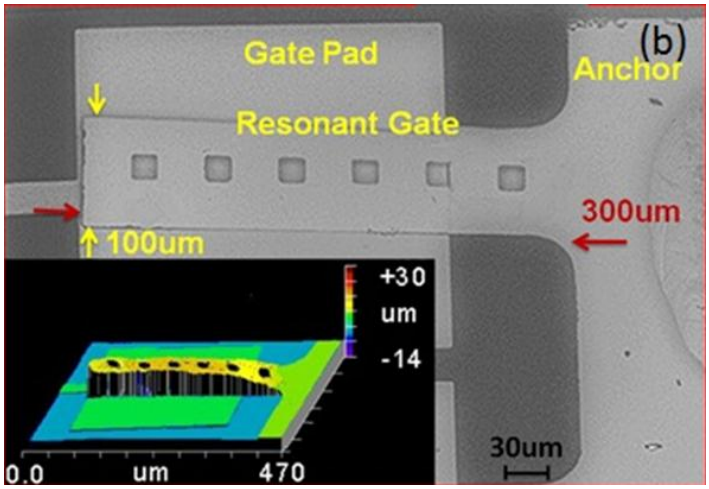


**Figure 3.1.** An image of the titanium/ Metglas® cantilever integrated in the Feng Li's MERGT magnetic sensor. The cantilever shown in this image is only 300 µm long, while the one used for the experiments presented in this thesis are 500 µm long. In the bottom left is a Zygo image demonstrating the gap between the cantilever and the gate. Taken from [3].

The first of two methods used for the readout of the cantilever sensors made use of a

position sensitive photodetector (PSD) to measure the deflections of a laser beam reflected off the tip of the cantilever directly corresponding to the deflections of the cantilever itself.

## 3.2 Position Sensitive Photo Detection

### 3.2.1: Position Sensitive Photo Detectors

PSD's are opto-electronic devices that take advantage of the photoelectric effect to continuously track the position of an incident light spot on the PSD. By dividing the PSD into two halves or four quadrants, one can track the 1-dimensional or 2-dimensional motion of the light spot respectively. For example, if a PSD is divided into two halves, then the PSD has two output currents: one for each half. By observing the relationship between these two output currents, the position of the light spot can be determined using the following equation:

$$Position = \frac{L}{2}\frac{Y_1 - Y_2}{Y_1 + Y_2}$$

where $L$ is the length of the PSD, $Y_1$ is the current from one half of the PSD, and $Y_2$ is the current from the other half of the PSD. This relationship can easily be extrapolated to working with a 2-dimensional PSD that as four quadrants with the following relationship:

$$Position\ y = \frac{L_y}{2}\frac{Y_1 - Y_2}{Y_1 + Y_2}$$
$$Position\ x = \frac{L_x}{2}\frac{X_1 - X_2}{X_1 + X_2}$$

where $L_y$ is the length of the PSD along the y-axis, $L_x$ is the length the of PSD along the x-axis, $X_1$ is the current from on half of the x-axis of the PSD, and $X_2$ is the current from the other half of the x-axis [8]. Illustrations of 1-dimensional and 2-dimensional PSD's are shown in Figure 3.2.

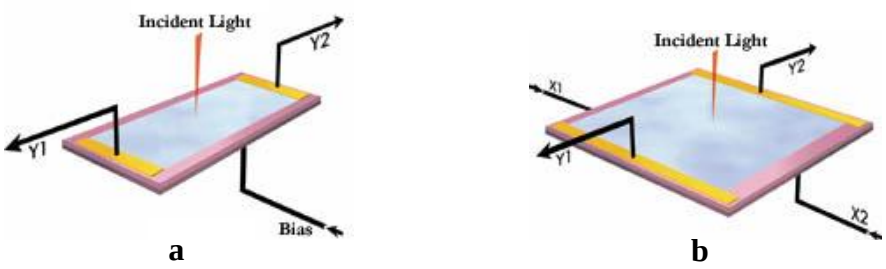


**Figure 3.2.** An illustration of the structure and functionality of a 1-dimensional PSD (**a**) and a 2-dimensional PSD (**b**). Taken from [7].

## 3.2.2: Optical Setup Implementation

The optical setup used to measure cantilever deflections with a PSD is composed of three primary components: a laser, a controlled magnetic field, and a data acquisition system. All of these components can be seen in Figure 3.3.

This optical setup uses lenses and mirrors to direct a 600 nm wavelength laser diode onto the tip of the cantilever to be observed. The laser is directed into a Sitek Electro-Optics 2-D PSD. The PSD feeds into a National Instruments data acquisition box, which is then input into the PC for data processing in Labview®. A screen shot of the Labview® interface is shown in Figure 3.5, where the significant data for this experiment can be found in the bottom left showing the voltage output of the PSD over time, which directly corresponds to cantilever deflections. An illustration of this laser diode deflection system is shown in Figure 3.4.

The small signal magnetic field is generated by a pair of Helmholtz coils with a time varying current. This time varying current is generated by applying a time varying voltage across the resistance of the two Helmholtz coils connected in series. A Hewlett Packard 3314A function generator is used, however, because of the 3314A's limited power output and the current requirements of the Helmhotz coils, the 3314A is used to drive a Hewlett Packard E3614A DC power supply, creating the effect of a high power function generator. The current through the coils is monitored by a Fluke 116 Multimeter and the magnetic field near the device being characterized is monitored by a Gauss meter.

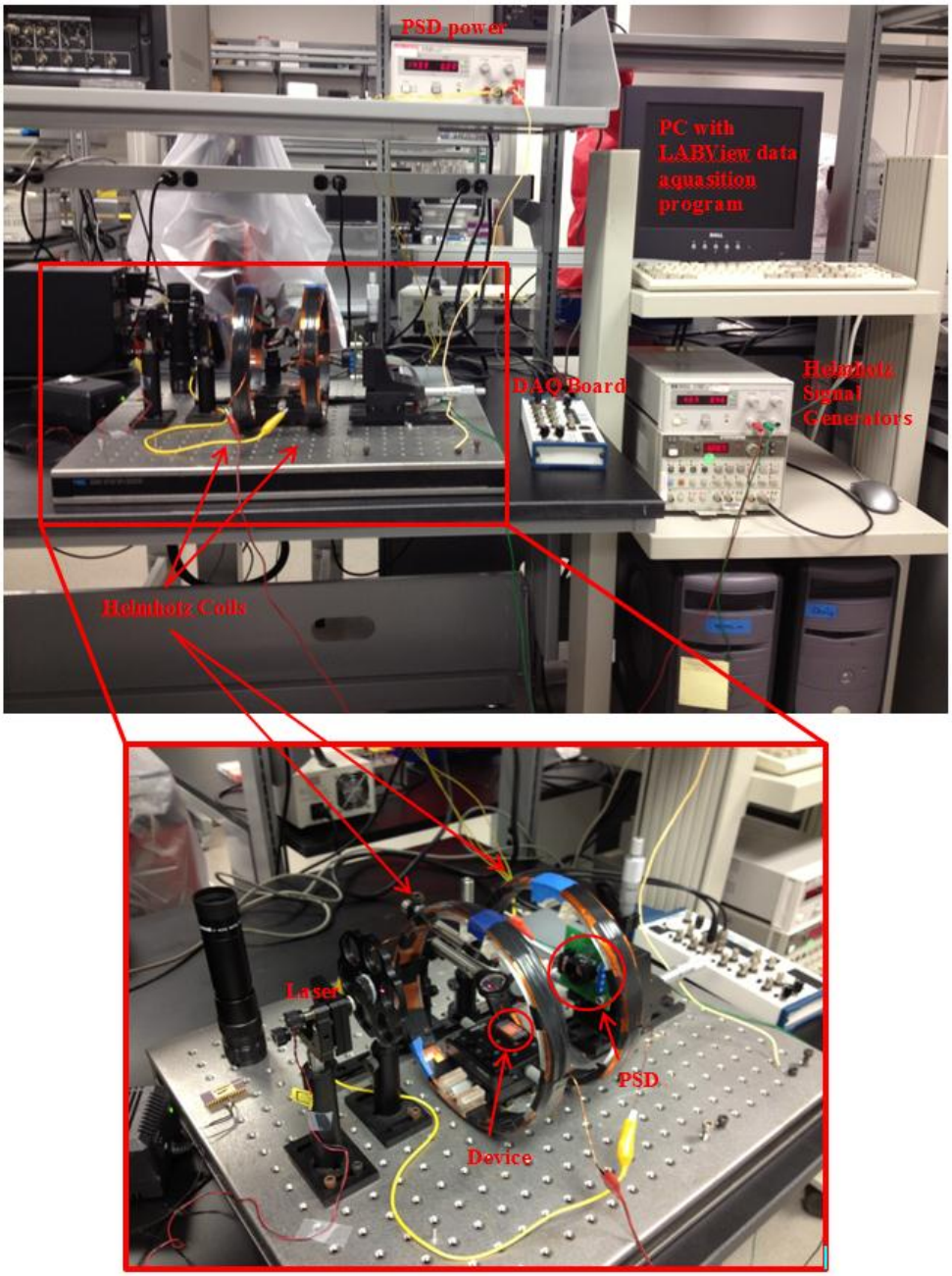


**Figure 3.3.** A photograph of the experimental setup used to measure cantilever deflections using a reflected laser diode and a PSD.

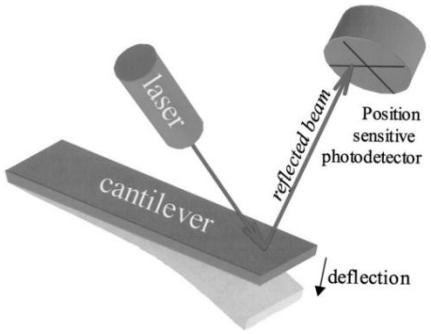


**Figure 3.4.** An illustration of the laser diode deflection method for measuring cantilever deflections with a PSD. Taken from [6].

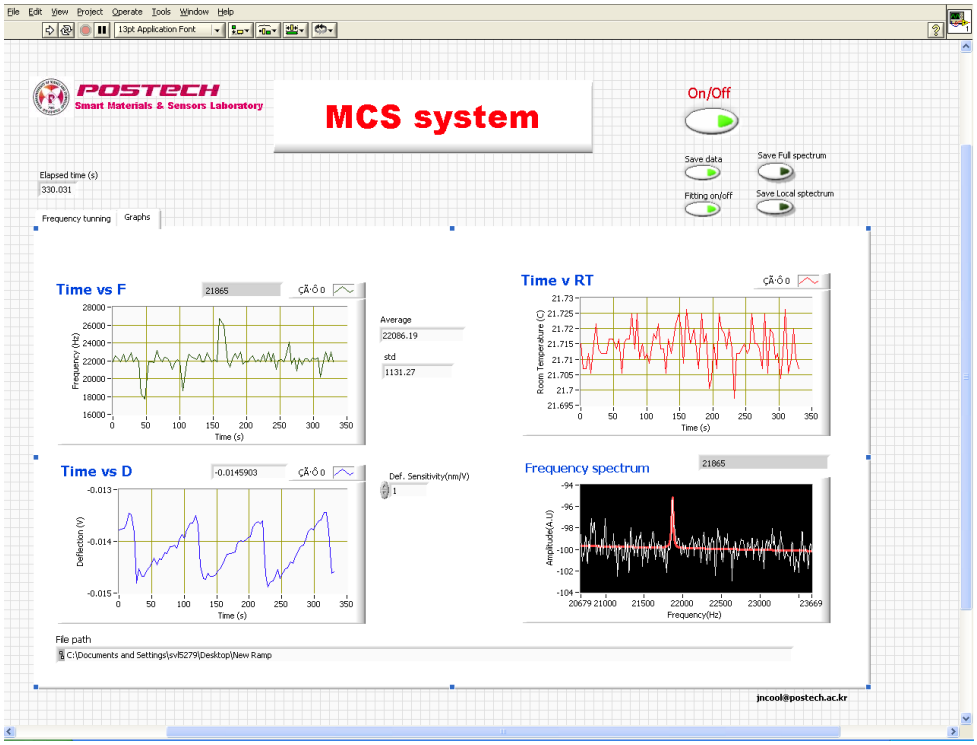


**Figure 3.5.** A plot of the Helmhotz coils' magnetic field as a function of applied

The specific experiment run on the cantilevers presented in this thesis uses the HP 3314A function generator outputting a triangle wave with 95%-5% symmetry at a frequency of 0.01 Hz, 5.95 $V_{pp}$, with an offset of 3.0 V. These seemingly arbitrary parameters are chosen to maximize the potential of the HP E3614A DC power supply (which is rated for 0-8 V, 0-6 A), and thus maximize the magnetic variation we can obtain with the Helmholtz coils. Driving the E3614A with the above function results in

an output of 0-9.27 V without any clipping of the E3614A. The current through the Helmholtz coils as a result of this driving voltage varies from 0-0.784 A, corresponding to a magnetic field varying from 0-11.85 Gauss respectively. The relationship between the voltage applied across the Helmholtz coils and the resultant magnetic field is plotted in Figure 3.6. It can be clearly seen that the magnetic field corresponds linearly to the applied voltage.

To explain the extremely slow frequency of the time varying magnetic field, we have to consider the functioning of the Labview® program. The program is designed to sample the PSD for about three seconds, average the data, and output the result. As a result, in order to view the displacement of the cantilever resulting from a time varying

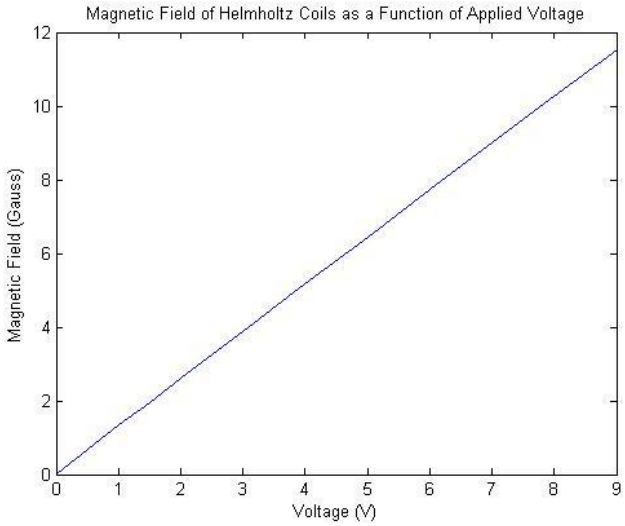


**Figure 3.6.** A screen capture of the Labview® interface used to collect data from the PSD.

magnetic field, we want to use an extremely slow magnetic signal to give the Labview® program time to recognize it.

## 3.2.3: Measurement Results

Applying the above setup, Figure 3.7 shows the data collected from the PSD by the Labview® program. Noise data was also taken on this PSD setup, and the original data results are shown in Figure 3.8. The noise data was taken at a much high frequency than the signal data, so a moving average was applied and the result is shown in Figure 3.9.

The root mean square (RMS) value of the average noise shown in Figure 3.9 is 59.916 μV, so we can calculate the signal to noise ratio (SNR) using the following equation:

$$SNR = \frac{Signal\ Strength}{RMS\ of\ noise}$$

For the case of this PSD setup, the SNR value is 71.9 V/V.

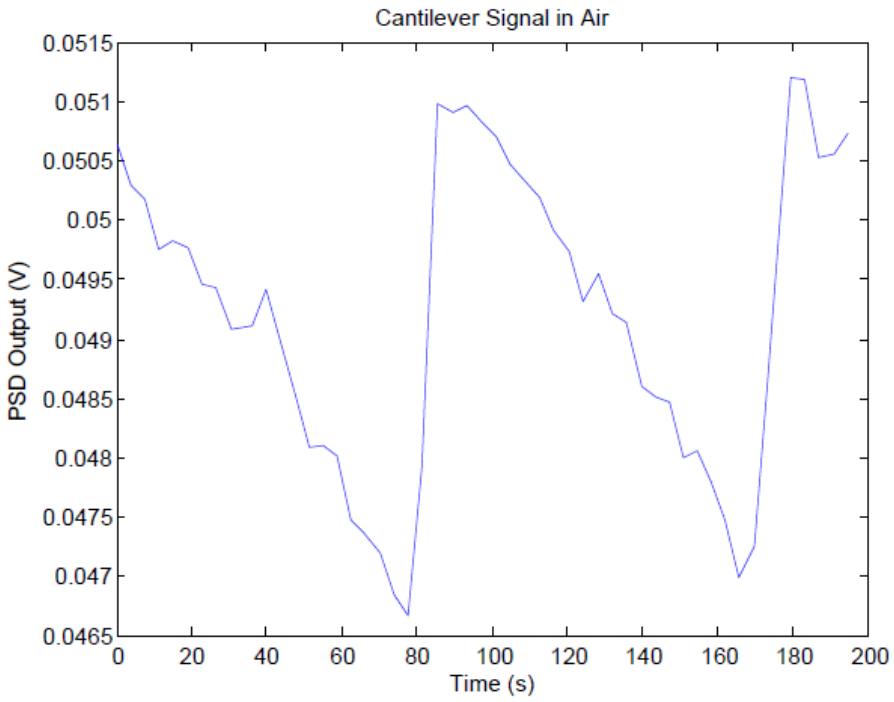


**Figure 3.7.** A plot of the cantilever's signal as measured by the PSD in response to the applied magnetic signal from the Helmholtz coils. The cantilever is in atmosphere.

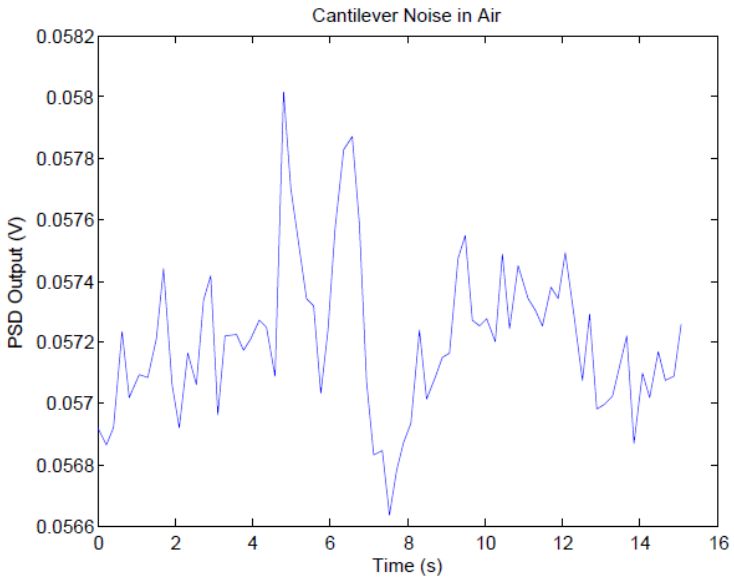


**Figure 3.8.** A plot of the cantilever's noise signal as measured by the PSD in response to the applied magnetic signal from the Helmholtz coils. The cantilever is in atmosphere.

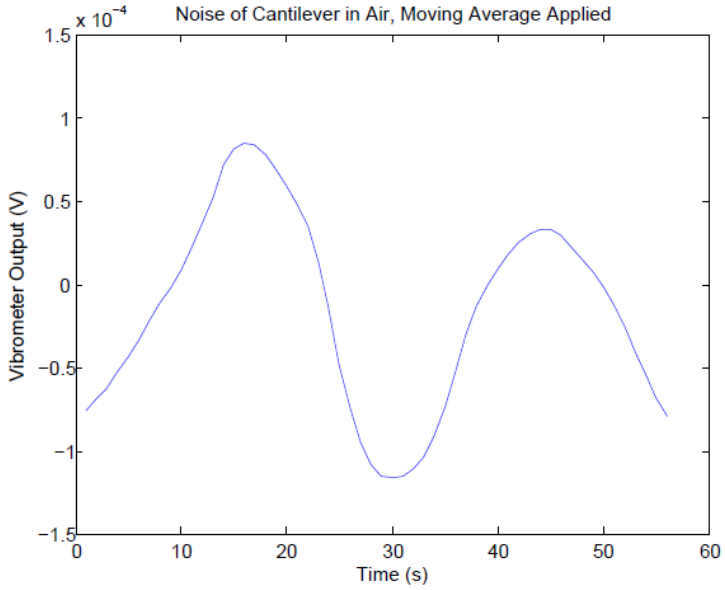


**Figure 3.9.** A plot of the moving average of the cantilever's noise signal as measured by the PSD in response to the applied magnetic signal from the Helmholtz coils. The cantilever is in atmosphere.

## 3.3: Vibrometer Detection

### 3.3.1: Laser Doppler Vibrometer

In this experiment, a single-point vibrometer is used to detect movement of the magnetostrictive cantilever. The function of a single-point vibrometer is to measure the the out-of-plane motion of a sample that is perpendicular to the laser beam used by the vibrometer. Practically, this simply means that the single-point vibrometer measures the amount of vibration at a single point on a sample's surface.

The physical principle used by the vibrometer to make measurements is a laser-Doppler vibrometer (LDV) that takes advantage of interferometry and the Doppler Effect to measure the displacement and velocity of a sample. As illustrated in Figure 3.10, the LDV works by first splitting a laser into a reference beam and a measurement beam. The reference beam always travels the same distance into the third beam splitter and then the detector, while the measurement beam continues on to the sample. The reflected measurement beam then returns to the LDV and is split by the second beam splitter, sending it toward the third beam splitter.

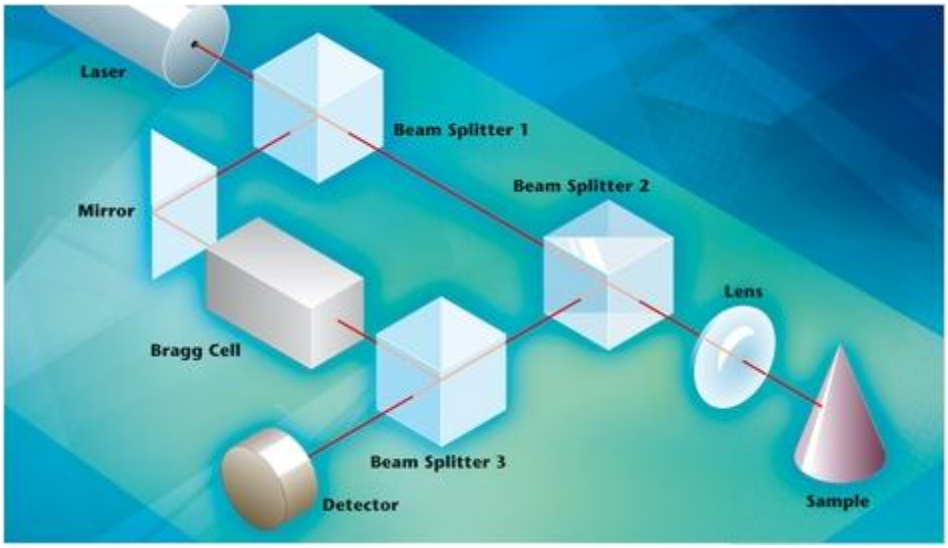


**Figure 3.10.** An illustration of a laser-Doppler vibrometer. Taken from [9]

What we are left with entering the detector is a reference beam that has traveled a known distance and a measurement beam whose travel distance is dependent upon the displacement of the sample. These two beams interfere with one another, creating a fringe pattern for the detector that results from the overlap of the two light intensities, as described by the following equation:

$$I_{tot} = I_1 + I_2 + 2\sqrt{I_1 I_2 \cos\left[\frac{2\pi(r_1 - r_2)}{\lambda}\right]}$$

where $I_1$ and $I_2$ are the intensities of the reference and measurement beam respectively, and $r_1$ and $r_2$ are the path lengths of the reference and measurement beam respectively. As the position of the sample moves, the fringe pattern changes correspondingly.

Similarly, the velocity of the sample is detected by the frequency shift caused by the Doppler Effect:

$$f_D = 2\frac{v}{\lambda}$$

Where $f_D$ is the Doppler frequency, $v$ is the velocity of the sample, and $\lambda$ is the wavelength of the original frequency. This shift in frequency also results in the fringe pattern changing accordingly [9].

### 3.3.2: Vibrometer Setup

The vibrometer setup used to measure cantilever deflections, similar to that of the PSD, is composed of three primary components: a vibrometer, a controlled magnetic field, and a data acquisition system. All of these components can be seen in Figure __.

This vibrometer setup uses a Polytec vibrometer composed of an OFV-534 compact sensor head and an OFV-5000 vibrometer controller. The data from the controller is collected by Labview® and saved as a text file. The small signal magnetic field is generated using the exact same Helmholtz coil setup and applied signal, but the frequency of the applied signal used with the vibrometer is 0.25 Hz. Data is collected in 30 second periods at a 40 kHz sampling frequency. Data was collected while the

cantilever sample was collected with the sample in atmosphere, however, an important advantage of the vibrometer setup over the PSD setup is that it also allowed for data to be collected in vacuum.

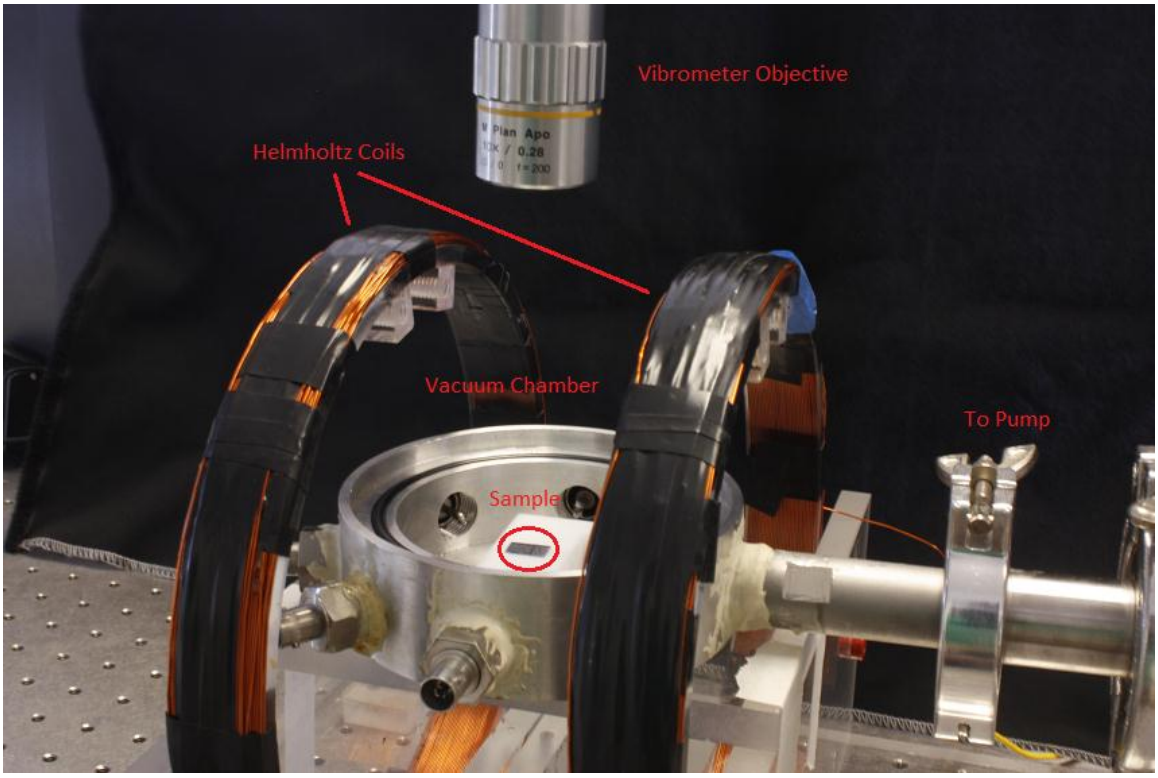


**Figure 3.11.** A photograph of the experimental setup used to measure cantilever deflections using a vibrometer.

### 3.3.3: Measurement Results

A plot of the data collected over a 30 second period with the device in atmosphere is shown in Figure 3.12. Magnetic signal from the Helmholtz coil is applied to the first 10 seconds, and the remaining 20 seconds have no signal applied and simply represent the noise of the cantilever in atmosphere. In order to extract the signal more clearly out of the raw data, a moving average filter was applied to the data, producing the plot in Figure 3.13. To obtain the signal to noise ratio, the magnitude of the signal, 15.39 mV, was taken from the last triangle in Figure 3.13. Because Figure 3.13 lacks a long period of noise, an additional set of data was collected with a long period of cantilever noise due to

atmosphere. This raw noise data is plotted in Figure 3.14, and the same moving average filter was applied to obtain the plot in Figure 3.15, whose RMS value is 1.00 mV. This gives us an SNR of 15.39 V/V.

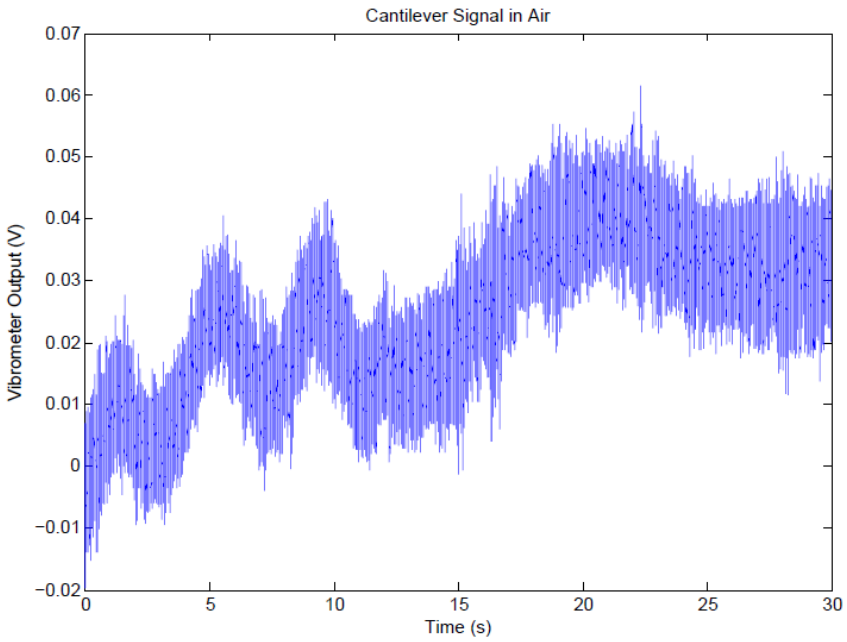


**Figure 3.12.** A plot of the cantilever's signal as measured by the vibrometer in response to 10 seconds of applied magnetic signal from the Helmholtz coils and 20 seconds of noise. The cantilever is in atmosphere.

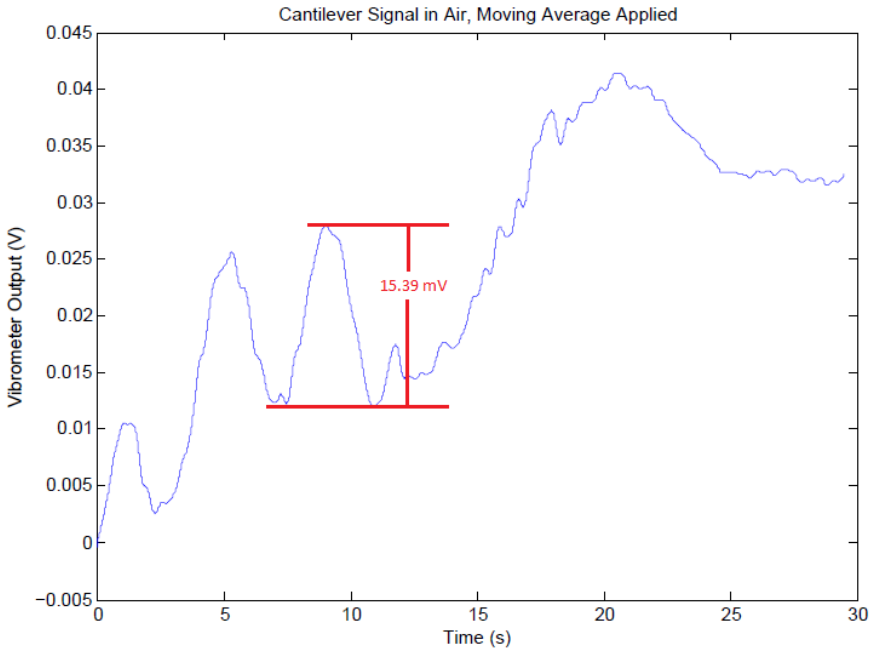


**Figure 3.13.** A plot of the moving average of the cantilever's signal as measured by the vibrometer in response to 10 seconds of applied magnetic signal from the Helmholtz coils and 20 seconds of noise. The cantilever is in atmosphere.

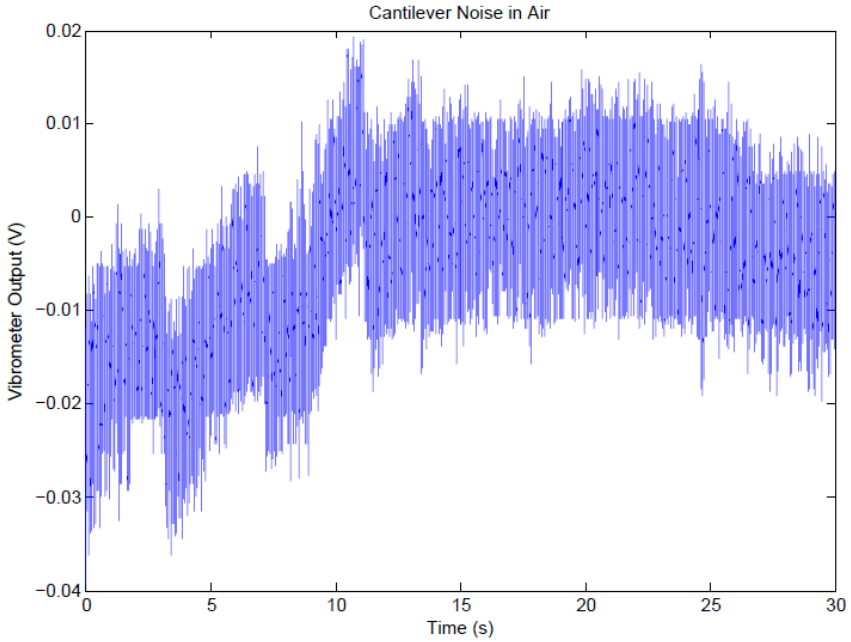


**Figure 3.14.** A plot of the cantilever's signal as measured by the vibrometer in response to 10 seconds of applied magnetic signal from the Helmholtz coils and 20 seconds of noise. The cantilever is in atmosphere.

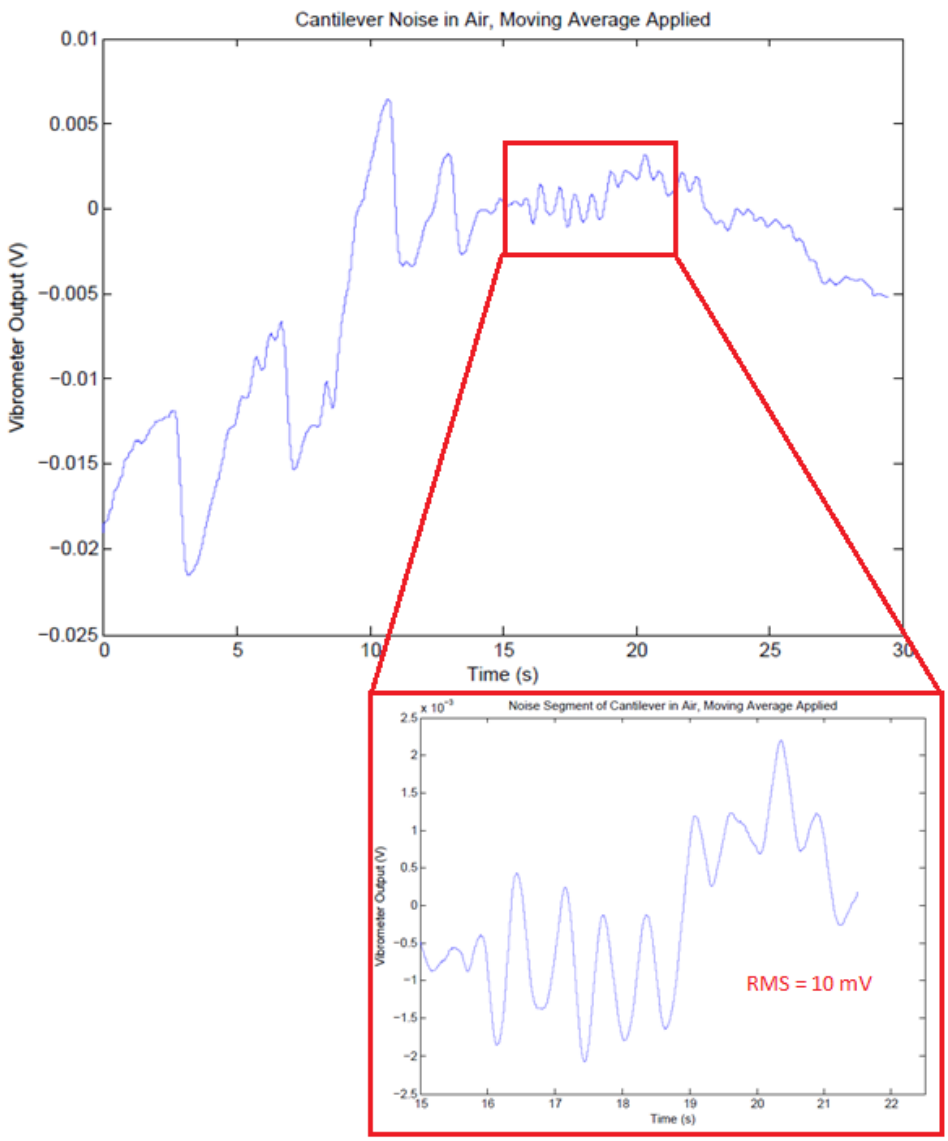


**Figure 3.15.** A plot of the moving average of the cantilever's signal as measured by the vibrometer in response to 10 seconds of applied magnetic signal from the Helmholtz coils and 20 seconds of noise. The cantilever is in atmosphere.

A plot of the data collected over a 30 second period with the device in vacuum is shown in Figure 3.16. The first 15 seconds have no signal applied and simply represent the noise of the cantilever in atmosphere, while the last 15 seconds have the applied magnetic signal. To obtain the signal to noise ratio, the magnitude of the signal, 26.03 mV, was taken from the last triangle wave in the second 15 seconds, while the first 15 seconds were corrected for the drift and used to find the RMS of the noise, 0.736 mV.

This gives us an SNR of 35.35 V/V.

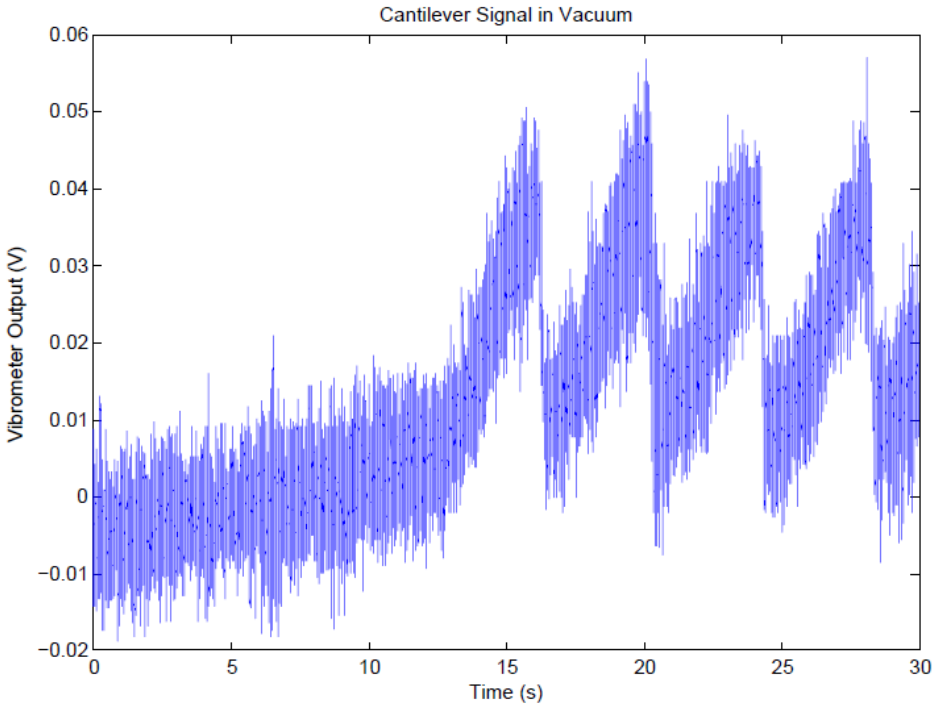


**Figure 3.16.** A plot of the cantilever's signal as measured by the vibrometer in response to 10 seconds of applied magnetic signal from the Helmholtz coils and 20 seconds of noise. The cantilever is in vacuum.

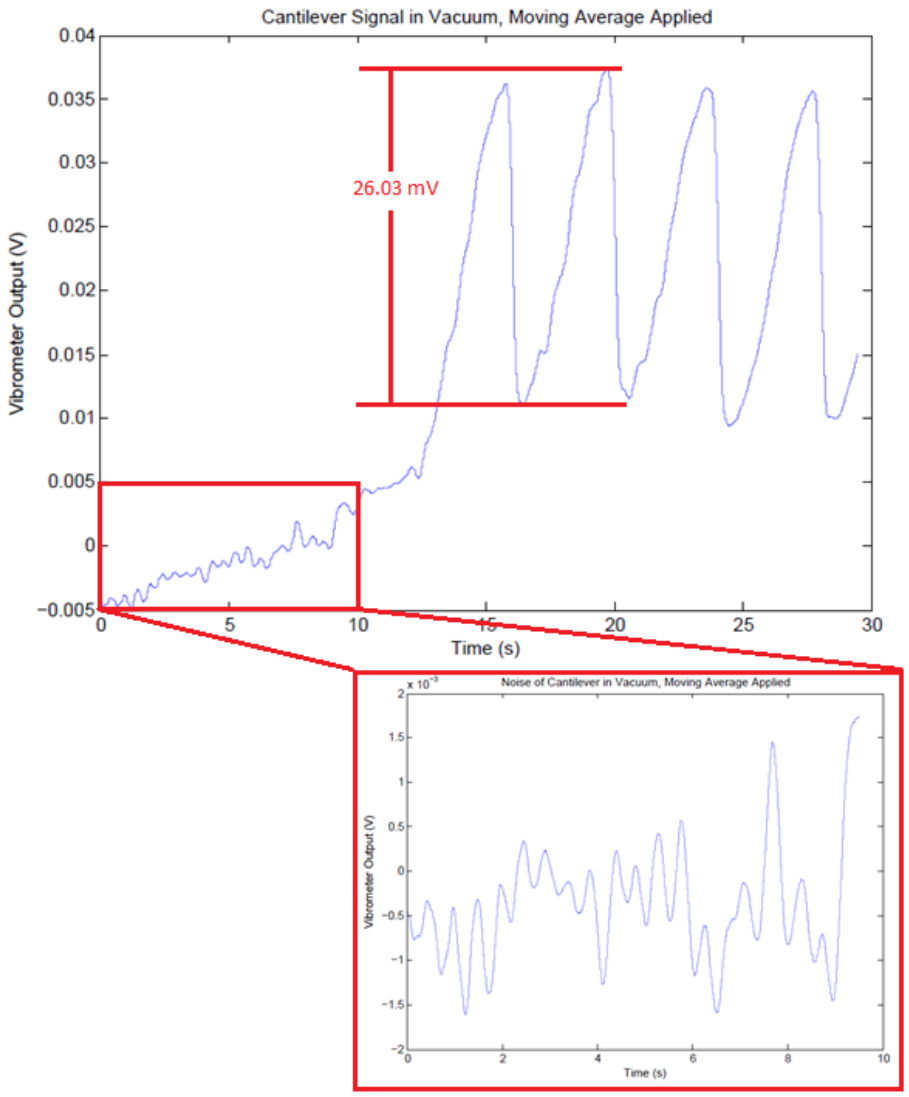


**Figure 3.17.** A plot of the moving average of the cantilever's signal as measured by the vibrometer in response to 10 seconds of applied magnetic signal from the Helmholtz coils and 20 seconds of noise. The cantilever is in vacuum.

## 3.4: Conclusions

The goal of this thesis was to provide evidence supporting the functionality of a unimorph Ti/ Metglas® cantilever being used in a MERGT magnetic sensor device. Over the course of this thesis, it was demonstrated that the unimorph cantilever responded linearly to an applied magnetic signal using two separate optical techniques: a custom

designed PSD detection setup and a vibrometer setup.

# Bibliography


[1] M. J. Caruso, T. Bratland, C. H. Smith, and R. Schneider, "A new perspective on magnetic field sensing,"

[2] H. Yabuki. Quasi-planar SNS junction as a sensor of brain studies. The Institute of Physical and Chemical Research. [Online]. Available: http://www.riken.go.jp/Yoran/BSIS/140B-141.html

[3] F. Li, R. Misra, Z. Fang, Y. Wu, Q. Zhang, P. Schiffer, S. Tadigadapa, and S. Datta, "Magnetoelectric resonant gate transistor with nanotesla sensitivity," submitted for publication in JMEMS, 2012.

[4] R. Nave. "Magnetostriction: Why does the transformer hum?" Internet: http://hyperphysics.phy-astr.gsu.edu/hbase/solids/magstrict.html, [7 April 2012].

[5] "Magnetostriction and Magnetostrictive Materials." Active Materials Laboratory. University of California in Los Angeles. Internet: http://aml.seas.ucla.edu/research/areas/magnetostrictive/mag-composites/Magnetostriction%20and%20Magnetostrictive%20Materials.htm, [7 April 2012].

[6] F. Li, R. Misra, Z. Fang, C. Curwen, Y. Wu, Q. M. Zhang, P. Schiffer, S. Tadigadapa, and S. Datta, "Magnetoelectric resonant gate transistor," Manuscript for Hilton Head 2012 Workshop.

[7] N. V. Lavrik, M. J. Sepaniak, and P. G. Datskos, "Cantilever transducers as a platform for chemical and biological sensors," *Review of Scientific Instruments*, vol. 75, pp. 2229-2253, 2004.

[8] "What's a PSD." Internet: http://www.sitek.se/, [7 April 2012].

[9] "Basic principles of vibrometry." Internet: http://www.polytec.com/us/solutions/vibration-measurement/basic-principles-of-vibrometry/, [7 April 2012].

# Academic Vita
# Christopher Curwen

**Name:** Christopher Curwen

**Address:** 5519 General Jenkins Drive
Mechanicsburg, PA 17050

**Email:** cac5378@gmail.com

**Education:**
The Pennsylvania State University, University Park, PA
B. S. in Electrical Engineering, May 2012

**Minor:** Physics

**Honors Thesis Title:** Optical Detection of Small Signal Magnetic Fields Using Magnetostrictive Cantilevers

**Thesis Advisor:** Srinivas Tadigadapa
Professor of Electrical Engineering

**Work Experience:**

**Power Engineering Trainee**
Electricity Authority of Cyprus, Summer 2010

**Research Experience for Undergraduates**
The Pennsylvania State University, Summer 2011

**Lab Assistant**
The Pennsylvania State University, January 2011 – May 2011

**Teaching Intern**
The Pennsylvania State University, August 2011 – May 2012

**Honors and Awards:**

Lockheed Martin Corporation Scholarship
President's Freshmen Award
Dean's List (all semesters)